

The open ocean energy decay of three recent trans-Pacific tsunamis

Alexander B. Rabinovich,^{1,2} Rogério N. Candella,³ and Richard E. Thomson²

Received 12 April 2013; revised 31 May 2013; accepted 31 May 2013; published 27 June 2013.

[1] The 2009 Samoa (M_w 8.1), 2010 Chile (8.8), and 2011 Tohoku (9.0) earthquakes generated destructive tsunamis recorded by a large number of DART stations in the Pacific Ocean. High-resolution (15 s) DART records yield mean energy decay times for these events of 17.3, 24.7, and 24.6 h, respectively. We attribute these differences to the frequency content of the tsunamis. Specifically, the Samoa tsunami was a “high-frequency” event with periods of 2–30 min whereas the Chile and Tohoku tsunamis were “broad-band” events with periods of 2–180 min. Differences in frequency content are linked to differences in the source parameters: Samoa was a relatively small deep-water earthquake while Chile and Tohoku were extensive shallow-water earthquakes. Frequency-dependent analysis of the Chile and Tohoku tsunamis indicates that shorter period waves attenuate much faster than longer-period waves (decay times range from 15 h for 2–6 min waves to 29 h for 60–180 min waves). **Citation:** Rabinovich, A. B., R. N. Candella, and R. E. Thomson (2013), The open ocean energy decay of three recent trans-Pacific tsunamis, *Geophys. Res. Lett.*, 40, 3157–3162, doi:10.1002/grl.50625.

1. Introduction

[2] Understanding tsunami energy decay in time and space is of primary scientific importance and critical for effective tsunami warning and mitigation. *Munk* [1963] suggested that tsunami energy in the ocean decays much like sound intensity does in an enclosed room. *Van Dorn* [1984, 1987] used this “acoustic analogy” to examine the attenuation of five major tsunamis and concluded, based on coastal measurements only, that the energy, $E(t)$, for all tsunamis decays as $E(t) = E_0 e^{-\delta t}$, where E_0 is the tsunami energy index, δ is the energy decay (attenuation) coefficient, and $t_0 = \delta^{-1}$ is the e -folding “decay time.” He found this decay to be event independent and nearly uniform for each ocean basin with $t_0 \approx 22$ h for the Pacific, 14.6 h for the Indian, and 13.3 h for the Atlantic oceans. Both *Munk* [1963] and *Van Dorn* [1984, 1987] postulated that the main energy losses are associated with absorption during multiple reflections from the mainland coasts at a rate of about e^{-1} per reflection. Thus, the decay time for each ocean was assumed to be of the order of mean “reflection” time defined as $t_r = L^*/c$, where $c = \sqrt{gH}$ is the

long-wave speed in mid-ocean, g is the gravitational acceleration, H is the mean water depth, and L^* is the mean travel path of tsunami waves.

[3] Early studies of tsunami decay were hampered by the small number and low quality of the analog pen-and-paper records available from coastal tide gauges at the time. The extensive high-quality data collected during the global 2004 Sumatra tsunami enabled *Rabinovich et al.* [2011] to use 173 coastal tsunami records to examine the tsunami energy decay in the Indian, Atlantic, and Pacific oceans. These results revealed that the decay time, t_0 , within a given oceanic basin is not uniform but depends on the absorption properties of the shelf adjacent to the observation site and on the travel time from the source region. Decay times for the 2004 Sumatra tsunami ranged from about 13 h for islands in the Indian Ocean near the source region to 40–45 h for remote mainland stations in the North Pacific, which is roughly twice the decay time of 22 h estimated by *Van Dorn* [1984, 1987] for the Pacific Ocean. The reasons for this difference in decay time were unclear and suggested the need for further investigation.

[4] Wave records from the 2009 Samoa, 2010 Chile, and 2011 Tohoku trans-Pacific tsunamis provide an excellent opportunity to re-visit the energy decay problem. In addition to originating from widely separated regions in the same ocean basin, the three tsunamis were the first to have been recorded by a large number of open-ocean Deep-ocean Assessment and Reporting of Tsunamis (DART) stations distributed throughout the entire Pacific Ocean. Wave records from these stations are free from regionally distorting topographic effects, making it possible to evaluate “pristine” tsunami decay times and to compare these times to the more data-limited estimates of *Munk* [1963], *Van Dorn* [1984, 1987] and *Rabinovich et al.* [2011].

2. Observations

[5] DART buoys operated by the U.S. National Atmospheric and Atmospheric Administration (NOAA) record seafloor bottom pressure at a sampling interval $\Delta t = 15$ s. In the absence of a tsunami event, these data are averaged internally to a default sampling interval $\Delta t = 15$ min and then transmitted every hour via satellite to the U.S. National Data Buoy Center. Upon sensing a tsunami event, DART begins to transmit the “raw” 15 s data directly for several minutes before the instrument switches to 1 min averages until the end of the event mode [*Moffeld*, 2009]. The 15 s tsunami data are stored in the instrument package and downloaded following instrument retrieval [*Mungov et al.*, 2013]. It is these retrieved 15 s datasets—consisting of 24 records for the 2009 Samoa, 23 for the 2010 Chile, and 18 for the 2011 Tohoku tsunamis—that we use for the present study. For the 2011 tsunami, we also made use of 11 “event” DART records, which were long enough to reliably estimate E_0 and t_0 . Figure 1 shows the specific DART stations used in

Additional supporting information may be found in the online version of this article.

¹P.P. Shirshov Institute of Oceanology, Moscow, Russia.

²Institute of Ocean Sciences, Sidney, British Columbia, Canada.

³Instituto de Estudos do Mar Almirante Paulo Moreira, Arraial do Cabo, Brazil.

Corresponding author: A. B. Rabinovich, P. P. Shirshov Institute of Oceanology, 36 Nakhimovsky Prosp., Moscow, 117997, Russia. (A.B.Rabinovich@gmail.com)

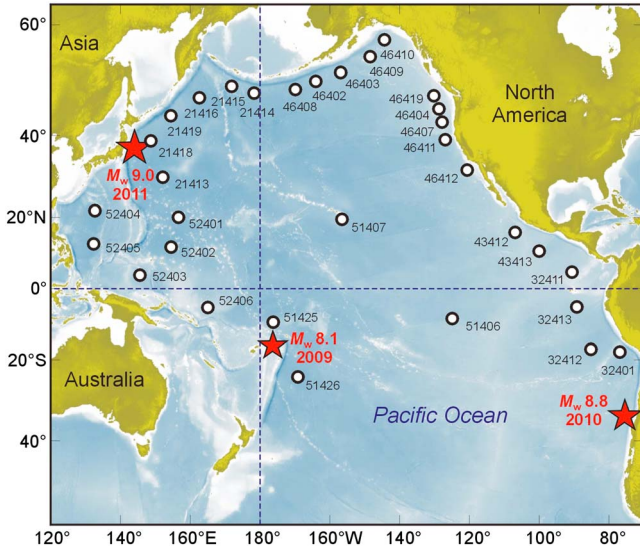


Figure 1. Map of the Pacific Ocean showing the location of the $M_w = 8.1$ 2009 Samoa, $M_w = 8.8$ 2010 Chile, and $M_w = 9.0$ 2011 Tohoku earthquake epicenters (stars) and positions of the DART open-ocean stations (circles).

our analyses. We first calculated the variance of each wave record based on 6 h data segments with 3 h overlaps. As illustrated by the examples in Figure S1 (see supporting information), the tsunami energy decayed exponentially with time. To evaluate the decay parameters E_0 and t_0 , we used least squares analysis to derive the best fit to the variance values. The record durations available to estimate these parameters ranged from 2.5 to 5 days and were dependent on how long the “ringing” of the tsunami signal was detectable above the background noise.

3. The 2009 Samoa Tsunami

[6] The $M_w = 8.1$ Samoa earthquake occurred at 17:48:10 UTC on 29 September 2009 [Lay et al., 2010]. The ensuing tsunami had a maximum runup on the Samoa coast of 17.6 m and was responsible for 189 fatalities [Okal et al., 2010]. The high-resolution (15 s) DART records from this event were used to estimate the tsunami parameters and to compare these parameters with numerical model results [Thomson et al., 2011]. Figure 2a shows maximum computed amplitudes for the 2009 tsunami waves and estimated E_0 values (see Table S1 of the supporting information for numerical values of the computed E_0 and t_0 estimates). According to these computations, the main “beam” of the tsunami energy was directed northeastward, toward the coast of Mexico. For other directions, the computed energy flux was approximately isotropic and yields E_0 values that are comparable with those obtained from the data for different DART sites. Minimum E_0 values of 0.15–0.20 cm^2 were observed at remote sheltered DARTs 52404, 21415, 21416, and 46408, while maximum values of 2.07–2.10 cm^2 were observed at more exposed DART sites 52401 and 51426 (see Figure 1 for DART locations); the mean value of E_0 , averaged over all DART records, was 0.80 cm^2 .

[7] The decay times derived from DART records for this event vary from $t_0 = 13.0$ –14.0 h at DARTs 21414, 46410, 51425, and 51426 to $t_0 = 22.8$ –24.2 h at DARTs 46408 and

52405. There appears to be a large-scale structure in the energy decay time. Specifically, the two DARTs (51425 and 51426) located in the vicinity of the source have $t_0 < 15$ h, while the “eastern DARTs” (located along the

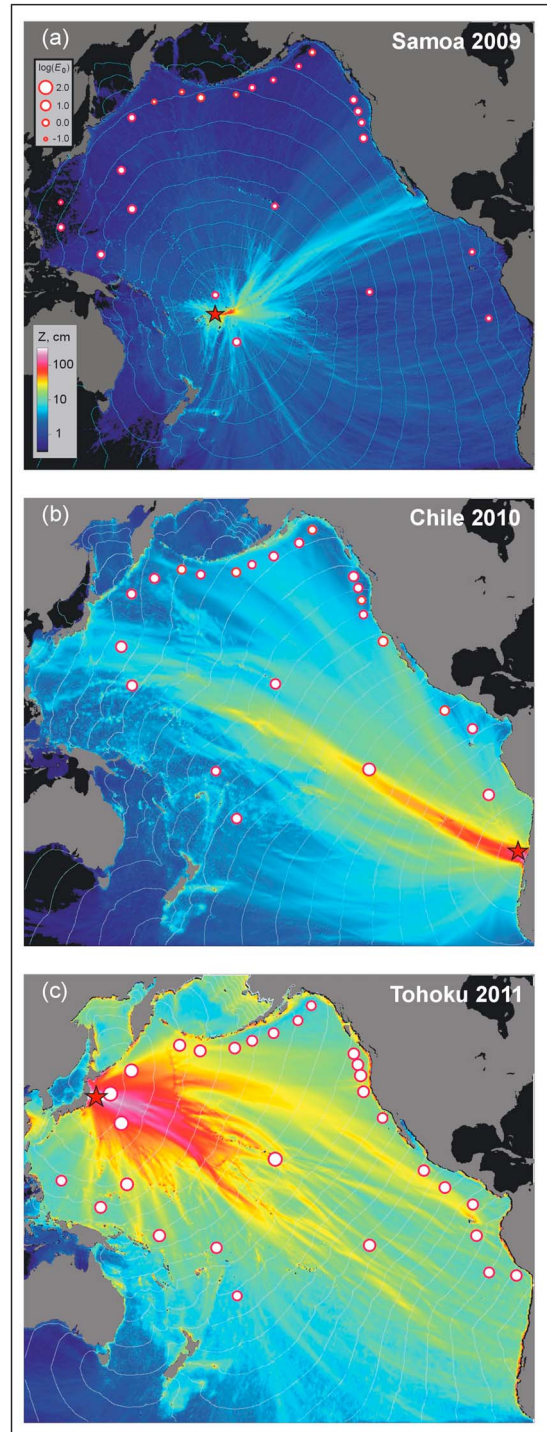


Figure 2. Simulated tsunami wave heights along with the tsunami wave energy indices, E_0 , for the (a) 2009 Samoa, (b) 2010 Chile, and (c) 2011 Tohoku tsunamis. Positions of the DART buoys are indicated by white circles, with the size of the circles proportional to E_0 . Red stars indicate the earthquake epicenters. Solid thin blue lines are hourly computed isochrones of tsunami travel time from the source areas.

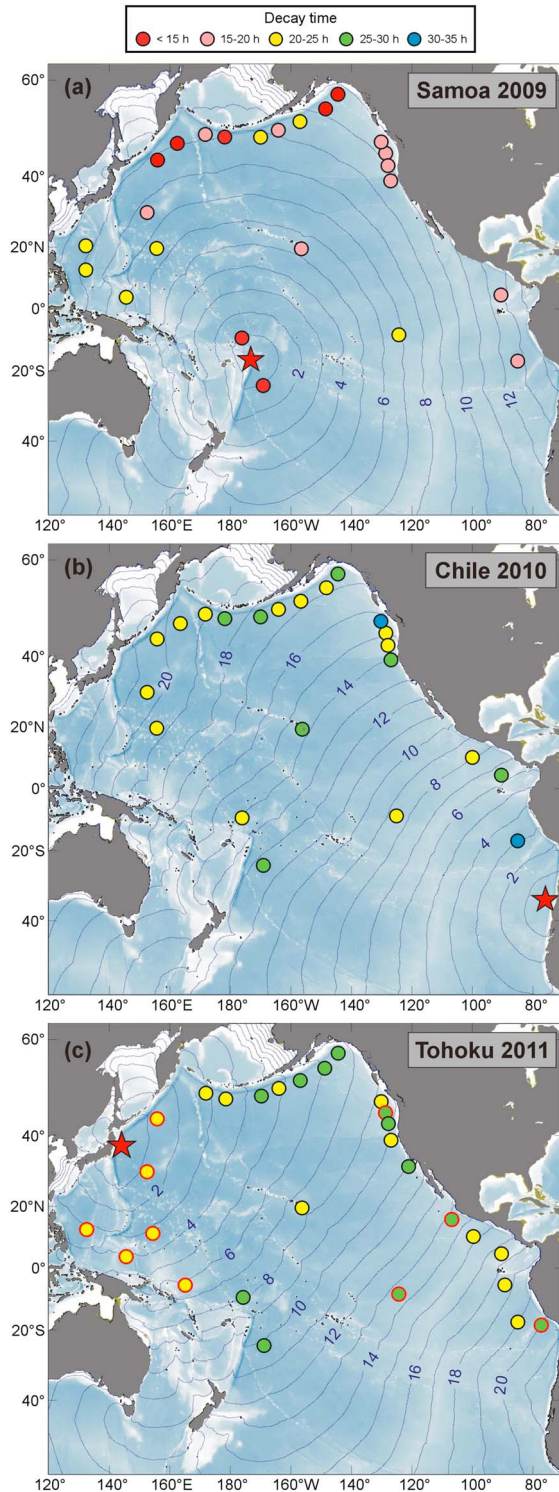


Figure 3. As in Figure 2, but for the energy decay times, t_0 , of the three tsunamis. Positions of DARTs are indicated by color circles; colors denote the tsunami decay time. Circles with red contours in Figure 3c indicate “event mode” DARTs with variable samplings.

coast of America) have $t_0 = 15\text{--}20\text{ h}$, and the “western DARTs” (located in the western Pacific) have mainly $t_0 = 20\text{--}25\text{ h}$ (Figure 3a). The mean value for all records was $t_0 = 17.3 \pm 0.7\text{ h}$.

4. The 2010 Chile Tsunami

[8] The 2010 tsunami event was generated by a magnitude $M_w = 8.8$ thrust-fault earthquake at 06:34 UTC on 27 February 2010 near the coast of Central Chile. The earthquake was the largest in the Southern Hemisphere since 1960 [Delouis *et al.*, 2010]. The resulting tsunami claimed 124 victims in coastal areas of Chile where the maximum observed tsunami runup was 29 m [Fritz *et al.*, 2011]. The tsunami was recorded by more than 200 coastal tide gauges and by many DART stations. Rabinovich *et al.* [2013] formulated a numerical model for this event that is in good agreement with the DART and tide gauge data. According to this model, the main beam of tsunami energy was directed northwestward toward the Marquesas and Hawaiian islands and Japan (Figure 2b); a substantial fraction of the tsunami energy was also directed northward to the coast of Mexico and California, in good agreement with observations [cf. Reymond *et al.*, 2013; Borrero and Greer, 2013]. The maximum estimated E_0 value of 44.0 cm^2 was obtained for DART 51406 located in the core of the main tsunami energy beam (Figure 2b); significant E_0 values of $12.8\text{--}17.6\text{ cm}^2$ were also obtained for other DART stations located to the northwest of the source (DARTs 32412, 52401, and 21413). In contrast, E_0 values were minimum ($2.1\text{--}2.9\text{ cm}^2$) at DART sites 46411, 46407, and 46410, which were outside the beams of the propagating wave field (Table S2, supporting information). The mean E_0 averaged over all 23 available DART records was 9.0 cm^2 , which is significantly larger than that for the 2009 Samoa tsunami, reflecting the fact that the 2010 earthquake and associated tsunami were much larger than for the 2009 event (note that the mean E_0 value for this event, as well as for the 2009 Samoa and 2011 Tohoku events, was strongly dependent on the availability of DART stations in the vicinity of the source).

[9] The estimated decay times for the 2010 Chile tsunami records vary from 28.6–28.1 h at DARTs 46419 and 32411 to 20.8–21.8 h at DARTs 46402 and 51406. In general, the more “western” DARTs have slightly shorter decay times than the “eastern” DARTs (Figure 3b). The mean value for the 23 DART records is $t_0 = 24.7 \pm 0.4\text{ h}$.

5. The 2011 Tohoku Tsunami

[10] At 05:46 UTC 11 March 2011, a giant thrust fault earthquake of magnitude $M_w 9.0$ occurred off the coast of Tohoku District, northeastern Honshu, Japan. The earthquake was the strongest in Japan’s history and one of the strongest ever instrumentally recorded [Simons *et al.*, 2011; Saito *et al.*, 2011]. Tsunami runup heights for this event were up to 40 m along the coast of Japan [cf. Mori *et al.*, 2011] and were responsible for almost 20,000 deaths. The 2011 tsunami was recorded by approximately 250 coastal tide gauges throughout the Pacific Ocean and by numerous bottom pressure gauges [cf. Song *et al.*, 2012; Saito *et al.*, 2011; Borrero and Greer, 2013]. The recorded data were used by Fine *et al.* [2013] and Tang *et al.* [2012] to examine tsunami energy propagation and transformation in the Pacific Ocean.

[11] We have estimated the energy decay parameters for the 2011 tsunami based on the 15 s records downloaded from 18 DART stations and “event mode” data obtained from 11 additional DARTs with various sampling intervals (Table S3, supporting information). Results from this

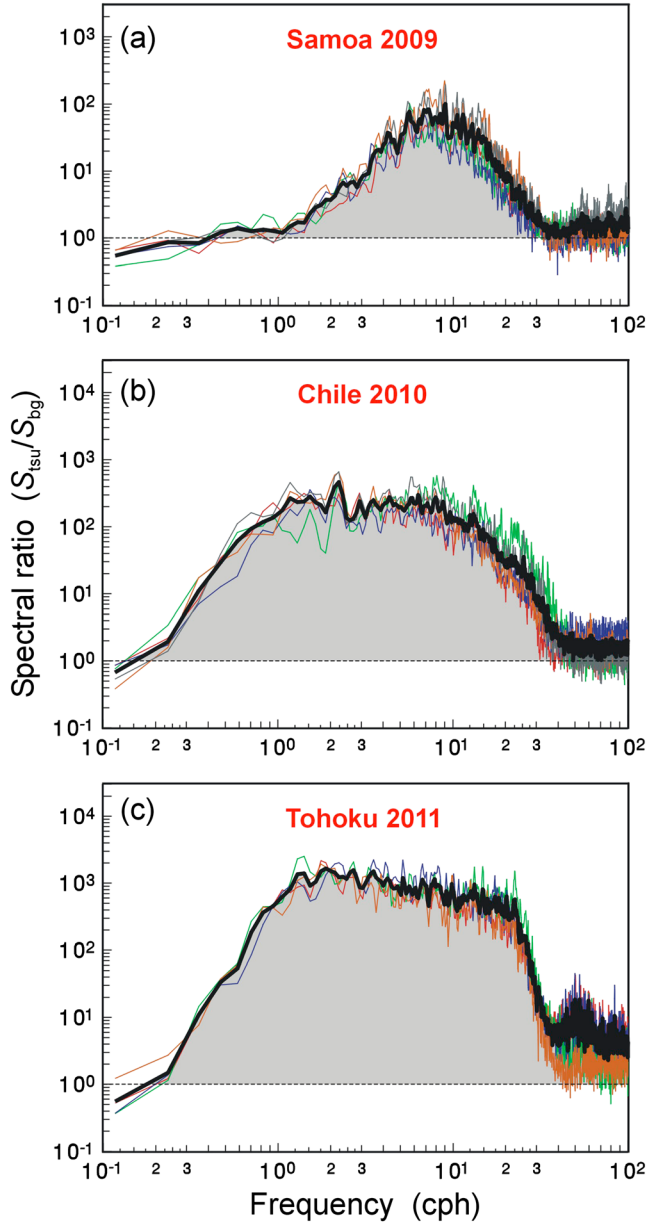


Figure 4. Estimated spectral ratios, $R_s(\omega)$ (tsunami/background), for the (a) 2009 Samoa, (b) 2010 Chile, and (c) 2011 Tohoku tsunamis. Individual color curves in plots are related to the mean value of $R_s^j(\omega)$ for the j th group of DARTs; thick black curves are the mean ratios, $\bar{R}_s(\omega)$, averaged over all available DART ratios (24 values for Figure 4a, 23 for Figure 4b, and 18 for Figure 4c). Shaded areas denote the mean tsunami response showing amplification of the tsunami wave spectra relative to the background wave spectra.

analysis are compared with the model results of *Fine et al.* [2013] (Figure 2c). According to the model, the tsunami energy flux was spread over a wide array of ray paths. The two main energy beams were directed eastward toward California and Mexico, and southeastward toward Peru and Chile. Two additional branches radiated northeastward toward the Aleutian Islands and southward to New Guinea and New Zealand. In general, there is good agreement between simulated and measured tsunami waves, as indicated by the strong coincidence between the computed beams of

maximum wave amplitude and sites with high recorded E_0 . The maximum tsunami energy was observed at DART 21418 ($E_0 = 161 \text{ cm}^2$) located close to the source area, at two nearby DART sites 21413 (127 cm^2) and 21419 (73 cm^2), and at DART site 51407 (93 cm^2) located within the main branch of the propagating tsunami energy (Figure 2c). The minimum value of E_0 ($6.0\text{--}7.0 \text{ cm}^2$) was found at DARTs 46409, 46410, and 51426 situated in remote corners of the DART network relative to the tsunami source. These results match well coastal observations of the 2011 tsunami [cf. *Reymond et al.*, 2013; *Borrero and Greer*, 2013]. The mean E_0 value for all 29 DART records was 31.9 cm^2 , which is roughly 3.5 times greater than for the 2010 Chile tsunami, consistent with the greater magnitude of the 2011 Tohoku earthquake.

[12] The decay times estimated for the 2011 Tohoku tsunami are shown in Figure 3c. These times are mutually consistent, with t_0 values varying from 29.3 h at DART 46409 to 20.9 h at DART 46419. As with the 2010 Chile tsunami, the “western” group of DART stations yields slightly shorter decay times than the “eastern” group (Figure 3c). The mean t_0 value for the 29 records was 24.6 ± 0.4 h, in close agreement with estimates by *Tang et al.* [2012] for three selected coastal stations: Kahului, Hawaii 21.2 h, Crescent City, California 23.5 h, and Adak, Aleutian Islands 20.9 h.

6. Discussion and Conclusions

[13] Our DART-based estimates of t_0 for the 2011 Tohoku and 2010 Chile tsunamis (24.6 and 24.7 h, respectively) are almost identical. However, these values differ significantly from the value $t_0 = 17.3 \pm 0.7$ h for the 2009 Samoa tsunami. Two basic questions arise from our analysis: (1) Why is the decay time t_0 for the 2009 Samoa tsunami considerably less than those for the 2010 Chile and 2011 Tohoku tsunamis? and (2) why is t_0 for the three recent trans-Pacific tsunamis much shorter than the corresponding value of t_0 for tsunami waves observed within the Pacific Ocean following the 2004 Sumatra tsunami [*Rabinovich et al.*, 2011]?

[14] The second question is straightforward to answer. All three tsunamis that we examined in the present paper originated in the Pacific Ocean and essentially remained in the Pacific where they dissipated due to shelf/coastal absorption processes. In this sense, the acoustic analogy of sound intensity in an enclosed room [*Munk*, 1963] is valid. In contrast, the 2004 Sumatra mega-tsunami originated in the Indian Ocean and then subsequently entered the Pacific Ocean through a variety of connecting passages [*Rabinovich et al.*, 2011]. The wave energy continued to enter the Pacific for several days, where it maintained a high energy level and effectively reduced the “natural” rate of tsunami decay.

[15] The answer to the first question is likely related to differences in the frequency content of the tsunami wave fields. To examine this assumption, we conducted spectral analyses of the 15 s tsunami records collected by the DART buoys and compared the resulting tsunami spectra, $S_{\text{tsu}}(\omega)$, with the background spectra, $S_{\text{bg}}(\omega)$, at each of the corresponding sites. For analysis of background signals, we used the 5 day period immediately preceding the tsunami arrival times, yielding $\nu = 64$ degrees of freedom; for the tsunami waves, we used 21.3 h periods immediately following the wave arrivals, for which $\nu = 14$. Following *Rabinovich* [1997], we calculated spectral ratios, $R_s(\omega) = S_{\text{tsu}}(\omega)/S_{\text{bg}}(\omega)$, which

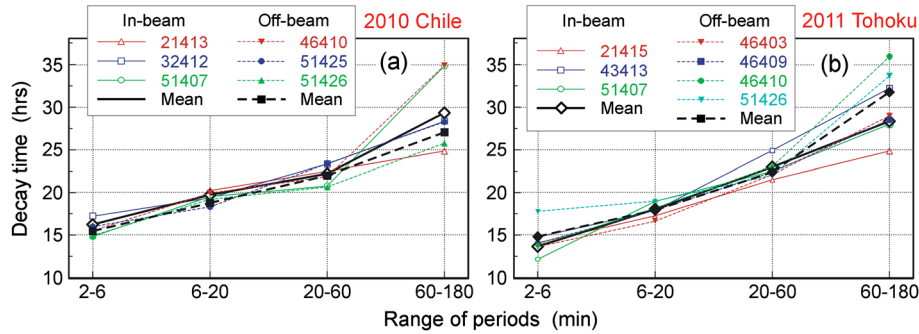


Figure 5. The tsunami decay time, t_0 , as function of wave period for the (a) 2010 Chile and (b) 2011 Tohoku tsunamis. The calculations are for two groups of stations: “in-beam” stations are those within the main beams of the tsunami energy propagation; “off-beam” stations are those outside the main beams.

give the amplification of the long-wave spectrum during the tsunami event relative to the background conditions. We began by estimating the mean regional values, $\bar{R}_s^j(\omega)$, for various groups of DARTs and then determining the mean ratios, $\bar{R}_s(\omega)$, averaged over all available DART records (Figure 4).

[16] Our findings show that the 2009 Samoa tsunami was a pronounced “high-frequency” event with periods ranging from 2 to 30 min and a distinct spectral peak at periods of 7–8 min. In contrast, the 2010 Chile and 2011 Tohoku tsunamis were “broad-band” events with periods ranging from 2 to 180 min and predominant low-frequency energy with periods in the range of 10–100 min (Figure 4). The differences in the wave frequency content appear to be related to the markedly different source parameters. In particular, the Samoa event was characterized by a relatively small-size deep-water source [Lay et al., 2010] whereas the Chile and Tohoku events were characterized by extensive shallow-water sources [cf. Delouis et al., 2010; Simons et al., 2011]. Rabinovich et al. [2011] argue that relatively small-scale, high-frequency tsunami wave components are absorbed more actively and decay more rapidly than larger-scale lower-frequency wave components.

[17] Following the suggestion of one of our reviewers, we examined the dependence of the time decay on wave frequency and the position of given DART stations with respect to tsunami energy beams. For the major events in 2010 and 2011, we selected two groups of DART stations: those “in-beam” and those “off-beam.” Each tsunami record was band-pass filtered to isolate wave oscillations in period ranges of 2–6, 6–20, 20–60, and 60–180 min (examples of the band-passed records are presented in Figure S2 of the supporting information). The filtered records were then used to estimate E_0 and t_0 for each range of periods (Figure 5; also Table S4 of the supporting information). Although we find no apparent difference between the in-beam and off-beam responses and, hence, no dependence of decay time, t_0 , on wave amplitude, there is a clear dependence of the decay time on wave period (Figure S3, supporting information). In particular, the estimates of $t_0 \sim 22$ h by Munk [1963] and Van Dorn [1984] closely correspond to the mean value $t_0 = 22.4$ h we obtain for the 20–60 min band. Longer period motions decay more slowly ($t_0 \sim 29.1$ h) than these historical estimates, while shorter (higher frequency) waves decay more rapidly ($t_0 \sim 15.1$ h, 2–6 min periods and ~ 18.6 h, 6–20 min periods). The latter estimates are in close agreement with our estimate $t_0 = 17.3$ h for the Samoa tsunami

which had typical wave periods of 2–20 min. The fundamental dependency of the decay times on wave frequency accounts for the markedly different rates of energy decay for the 2009 and 2010–2011 tsunamis.

[18] It is safe to assume that the effects of irregular bottom topography and coastal geometry cause tsunamis originating from different source regions in the Pacific Ocean to undergo different rates of energy dissipation. It is also apparent that extensive shallow-water shelves serve as energy “sinks,” actively absorbing and dissipating tsunami energy [Rabinovich et al., 2011]. Shelves and coastal resonance might also influence energy decay in offshore regions. However, regardless of the particular subtleties associated with each particular event, the results of the present study suggest that there is an underlying, universal decay rate linked to the frequency content of the original tsunami wave field in the Pacific Ocean.

[19] **Acknowledgments.** We thank Isaac Fine (Institute of Ocean Sciences, Sidney, Canada) for making available the results of his numerical models and for his helpful discussions, and George Mungov (NOAA, NGDC, Boulder, CO) for providing us with the retrieved high-resolution DART data. We thank Dominique Reymond for his valuable comments and one anonymous reviewer for his/her insightful suggestions regarding frequency-dependent energy decay. Work on this by ABR was partly supported by RFBR grants 12-05-00733-a and 12-05-00757-a.

References

Borrero, J. C., and S. D. Greer (2013), Comparison of the 2010 Chile and 2011 Japan tsunamis in the far field, *Pure Appl. Geophys.*, *170*, 1249–1274, doi:10.1007/s00024-012-0559-4.

Delouis, B., J. M. Nocquet, and E. M. Valle (2010), Slip distribution of the February 27, 2010 $M_w = 8.8$ Maule earthquake, central Chile, from static and high-rate GPS, InSAR, and broadband teleseismic data, *Geophys. Res. Lett.*, *37*, L17305, doi:10.1029/2009GL043899.

Fine, I. V., E. A. Kulikov, and J. Y. Cherniawsky (2013), Japan's 2011 tsunami: Characteristics of wave propagation from observations and numerical modelling, *Pure Appl. Geophys.*, *170*, 1295–1307, doi:10.1007/s00024-012-0555-8.

Fritz, H. M., et al. (2011), Field survey of 27 February 2010 Chile tsunami, *Pure Appl. Geophys.*, *168*(11/12), 1989–2010, doi:10.1007/s00024-011-0283-5.

Lay, T., C. J. Ammon, H. Kanamori, L. Rivera, K. D. Koper, and A. R. Hutko (2010), The 2009 Samoa–Tonga great earthquake triggered doublet, *Nature*, *466*, 964–968, doi:10.1038/nature09214.

Mofjeld, H. O. (2009), Tsunami measurements, in *The Sea*, vol. 15, *Tsunamis*, edited by A. Robinson and E. Bernard, pp. 201–235, Harvard Univ. Press, Cambridge, Mass.

Mori, N., T. Takahashi, T. Yasuda, and H. Yanagisawa (2011), Survey of 2011 Tohoku earthquake tsunami inundation and run-up, *Geophys. Res. Lett.*, *38*, L00G14, doi:10.1029/2011GL049210.

- Mungov, G., M. Eblé, and R. Bouchard (2013), DART® tsunameter retrospective and real-time data: A reflection on 10 years of processing in support of tsunami research and operations, *Pure Appl. Geophys.*, *170*, doi:10.1007/s00024-012-0477-5.
- Munk, W. H. (1963), Some comments regarding diffusion and absorption of tsunamis, in *Proceeding of the Tsunami Meeting, X Pacific Science Congress, IUGG Monogr.*, vol. 24, pp. 53–72, IUGG Paris.
- Okal, E. A., et al. (2010), Field survey of the Samoa tsunami of 29 September 2009, *Seismol. Res. Lett.*, *81*, 577–591.
- Rabinovich, A. B. (1997), Spectral analysis of tsunami waves: Separation of source and topography effects, *J. Geophys. Res.*, *102*(C6), 12,663–12,676.
- Rabinovich, A. B., R. Candella, and R. E. Thomson (2011), Energy decay of the 2004 Sumatra tsunami in the world ocean, *Pure Appl. Geophys.*, *168*(11), 1919–1950, doi:10.1007/s00024-01-0279-1.
- Rabinovich, A. B., R. E. Thomson, and I. V. Fine (2013), The 2010 Chilean tsunami off the west coast of Canada and the northwest coast of the United States, *Pure Appl. Geophys.*, *170*, doi:10.1007/s00024-012-0541-1.
- Reymond, D., O. Hyvernaud, and E. A. Okal (2013), The 2010 and 2011 tsunamis in French Polynesia: Operational aspects and field surveys, *Pure Appl. Geophys.*, *170*, 1169–1187, doi:10.1007/s00024-012-0485-5.
- Saito, T., Y. Ito, D. Inazu, and R. Hino (2011), Tsunami source of the 2011 Tohoku-Oki earthquake, Japan: Inversion analysis based on dispersive tsunami simulations, *Geophys. Res. Lett.*, *38*, L00G19, doi:10.1029/2011GL049089.
- Simons, M., et al. (2011), The 2011 magnitude 9.0 Tohoku-Oki earthquake: Mosaicking the megathrust from seconds to centuries, *Science*, *332*(6036), 1421–1425, doi:10.1126/science.1206731.
- Song, Y. T., I. Fukumori, C. K. Shum, and Y. Yi (2012), Merging tsunamis of the 2011 Tohoku-Oki earthquake detected over the open ocean, *Geophys. Res. Lett.*, *39*, L05606, doi:10.1029/2011GL050767.
- Tang, L., et al. (2012), Direct energy estimation of the 2011 Japan tsunami using deep-ocean pressure measurements, *J. Geophys. Res.*, *117*, C08008, doi:10.1029/2011JC007635.
- Thomson, R., et al. (2011), Observation of the 2009 Samoa tsunami by the NEPTUNE-Canada cabled observatory: Test data for an operational regional tsunami forecast model, *Geophys. Res. Lett.*, *38*, L11701, doi:10.1029/2011GL046728.
- Van Dorn, W. G. (1984), Some tsunami characteristics deducible from tide records, *J. Phys. Oceanogr.*, *14*, 353–363.
- Van Dorn, W. G. (1987), Tide gage response to tsunamis. Part II: Other oceans and smaller seas, *J. Phys. Oceanogr.*, *17*, 1507–1516.